Research Article

Melatonin attenuates cardiac injury caused by chromium-mediated oxidative stress in male Wistar rats: involvement of antioxidative mechanisms

Priyanka Ghosh[1], Tiyasa Dey[1], Romit Majumder[2], Madhuri Datta[2], Aindrila Chattopadhyay[2], Debasish Bandyopadhyay[1*]

[1]Oxidative Stress and Free Radical Biology Laboratory, Department of Physiology, University of Calcutta, 92, APC Road, Kolkata-700009, India
[2]Department of Physiology, Vidyasagar College, 39, Sankar Ghosh Lane, Kolkata-700006, India
*****Correspondence: debasish63@gmail.com, dbphys@caluniv.ac.in, Tel: +91 9433072066

Running title: Melatonin protects chromium-induced cardiac injuries

Received: December 22, 2022; Accepted: February 14, 2023

ABSTRACT

Cardiovascular disease (CVD) is a global health concern due to its high mortality. Heavy metals are the potential risk factor for CVD. Among other heavy metals, chromium (Cr) is considered a serious threat to human health due to its high oxidative capacity. In the current study, male Wistar rats were treated with Cr to induce cardiac tissue injuries, meanwhile, melatonin was given to test whether this treatment can protect against Cr-induced cardiac damage. The results showed that Cr markedly altered the heart weight, biomarkers of oxidative stress, activities of antioxidant and pro-oxidant enzymes, as well as tissue morphology. On contrary, melatonin treatment significantly suppressed all these alterations via its antioxidant activity. In addition, melatonin also significantly reduced tissue Cr concentration probably through its metal-chelating activity. The current study has demonstrated that melatonin is a promising antioxidant to protect the heart from Cr-induced oxidative damage, confirming that melatonin can be a future therapeutic agent for Cr-mediated toxicity in the heart or other organs.

Key words: cardiovascular disease, chromium, oxidative stress, ROS, cardiac injuries, antioxidant, melatonin

---

1. INTRODUCTION

Among all non-communicable diseases, cardiovascular diseases (CVDs) become a serious threat to human health. According to the report from World Health Organization (WHO-2019), CVDs are the leading cause of death globally. An estimated 17.9 million individuals died from CVDs per year worldwide (1). Besides many known causative factors, environmental pollutants are a significant but unrecognized one for the onset and progression of CVDs (2). Heavy metals are the most predominant environmental contaminants because they persist in the environment for a long time with continuous toxicity (3). Therefore, they are considered systemic toxicants leading to multiple organ damage even at lower concentrations (4).

Among them, chromium (Cr) has become a public concern due to its substantial utilization both industrially and civilly. Persons are occupationally exposed to Cr by working in industries of stainless steel, chrome plating, welding, mining, dyes and pigments, leather tanning, photography, and wood preservation (5) and also can be exposed by the consumption of contaminated food, water, and airborne dust or aerosols (6). The amount of Cr in ambient air and ground-water is relatively high in several places, including Europe (Belgium and Poland), Egypt (Cairo, Alexandria), the United States (North Carolina, New Jersey), Australia (Sydney), and India (Kanpur, Delhi, Agra, Lucknow, and Kolkata) (7, 8). According to a recent report, chromite ore mining is dominated in South Africa, followed by Kazakhstan, India, Turkey, and other countries (9). Cr has many oxidation states, but trivalent (III) and hexavalent (VI) are the most dominants. Cr (III) is used as a dietary supplement, whereas, Cr (VI) has carcinogenic, genotoxic, and mutagenic activities (10). Cr (VI) is non-biodegradable and thus can persist in water and soil for an extended period of time (11). It causes various disorders including allergic dermatitis, lung cancer, gastrointestinal (GI) dysfunction, liver and kidney diseases, neurotoxicity, and immunotoxicity (12, 13). Cr (VI) is readily absorbed in the gut and it crosses the cell membrane via anionic chloride phosphate and sulfate carriers (14). In the intracellular environment, Cr (VI) is converted to Cr (III), an event often recognized to produce hazardous consequences (15). Being redox-active, Cr (VI) may undergo Fenton and Haber-Weiss type of reactions to generate reactive oxygen species (ROS) including superoxide anion ($O^{2.-}$), hydroxyl radical ($^{\bullet}HO$), and hydrogen peroxide (H_2O_2) (16). When Cr (VI) binds to both non-enzymatic (GSH, Ascorbate) (17) and enzymatic antioxidants (NADPH/NADH-linked enzymes, electron transport chain [ETC] enzymes) (18), it produces a significant amount of ROS, which ultimately compromise the antioxidant defense system leading to damage of lipid, protein, DNA, and other biological structures (19, 20). Antioxidant supplements or consuming antioxidant-rich foods may provide beneficial effects in combating oxidative stress caused by Cr (VI). In this respect, melatonin seems to be a suitable molecule due to its potent antioxidative and metal-chelating properties (21, 22). Moreover, there is a strong inverse relationship between melatonin and heart disease, as it influences different cardiac events (23). This pineal indoleamine can directly detoxify ROS/RNS while it also boosts the activities of antioxidant enzymes or suppressed pro-oxidant enzymes (24, 25). These actions are mediated by receptors or receptor-independent (26). Melatonin is synthesized in the pineal gland but it can also be produced in the extra-pineal sites including the retina, lens, skin, gastrointestinal tract, liver, kidney, thyroid, pancreas, thymus, and spleen (27). It is also present in foodstuffs such as cereals and millet, vegetables, fruits, nuts, seeds, and herbs (28, 29). Consumption of melatonin-rich foods raises the blood level of melatonin in humans (30). It appears feasible to include melatonin in a dietary regimen targeting various diseases related to oxidative stress.

Thus, the current study aims to evaluate the efficiency of melatonin in alleviating cardiac tissue injury induced by Cr-mediated oxidative stress in male Wistar rats. The potential mechanisms are also explored.

2. MATERIALS AND METHODS

2.1. Chemicals.

The kits for the estimation of SGOT and CKMB were procured from Arkray Healthcare Pvt. Ltd. Sodium dichromate dihydrate ($Na_2Cr_2O_7.2H_2O$), melatonin, trichloroacetic acid (TCA), 5, 5'- dithiobis-2-nitrobenzoic acid (DTNB), bovine serum albumin (BSA), nicotinamide adenine dinucleotide phosphate reduced and oxidized (NADPH and $NADP^+$), reduced glutathione (GSH), nitro blue tetrazolium (NBT), sodium pyruvate ($CH_3COCOONa$)

and other necessary reagents were purchased from Sisco Research Laboratories, (Mumbai, India). Nicotinamide adenine dinucleotide (NAD^+), glutathione oxidized (GSSG), phenazine methosulfate (PMS), o-phenylenediamine dihydrochloride (OPD), and other chemicals were purchased from Sigma Aldrich Merck (St. Louis, Missouri; USA). Thiobarbituric acid (TBA) and other chemicals were purchased from Merck Limited, (Delhi, India). All chemicals used in different assays were of analytical grade purity.

2.2. Animals.

Male Wistar rats weighing 180 ± 10g (age 3-4 months) were obtained from a CPCSEA-registered supplier and handled throughout the experiment as per the guidelines from the Committee on Prevention of Cruelty and Supervision of Experiments on Animals (CPCSEA) under the Ministry of Social Justice and Empowerment, Government of India. The rats were kept in well-ventilated polypropylene cages in the departmental animal house under controlled environmental conditions of temperature (25 ± 1°C), humidity (50 ± 10%), and light: dark cycle (12:12 h). They had free access to food and drinking water *ab libitum.* The animals were acclimatized to laboratory conditions for 5 days before starting experiments. All the experimental protocols were approved by the Institutional Animal Ethics Committee (IAEC) [Approval number: IAEC-V/T/DB-3(Priyanka Ghosh)/2019 dated 7.8.19] of the Department of Physiology, University of Calcutta.

2.3. Experimental Design.

After acclimatization, the animals were divided into ten different groups (n=4) and subjected to the following treatment schedule (Figure 1):

1**.** *Control groups (Con):* The animals were subcutaneously (s.c.) given a vehicle for 7 (Con 7) or 14 (Con 14) days, respectively for each Con groups.

2. *Chromium-treated groups (Cr):* The animals were subjected to subcutaneous injection of Cr at the dose of 5 mg/kg body weight (b.w) (31) on alternate days for 7 (Cr7) or 14 (Cr14) days, respectively for each Cr groups.

3. *Melatonin-treated groups (M):* The animals were administered with melatonin by gavage, at the doses of 5 (M5), 10 (M10), or 20 (M20) mg /kg b.w. for 14 days, respectively for each M groups.

4. *Chromium + melatonin co-treated group (CrM):* The animals were administered with melatonin by gavage for 30 minutes at the doses of 5 (CrM5), 10 (CrM10), and 20 (CrM20) mg/kg b.w. respectively, before subcutaneous injection of Cr (5mg/kg b.w.). Melatonin treatment was continued for a period of 14 days, respectively for each CrM groups.

2.4. Sample collection.

Animals were fasted overnight at the end of the treatment period. Following intraperitoneal injection of a specific dose of ketamine hydrochloride, the rats were sacrificed through cervical dislocation according to CPCSEA guidelines. The abdomen and chest compartments were carefully opened, and blood was collected through cardiac puncture. The collected blood was stored overnight to allow coagulation for serum collection. The serum was kept at -20°C for subsequent assays. The heart was removed, washed in cold saline, soaked with blotting paper, and preserved in sterile plastic vials. The tissues were kept at -20°C for future assay.

2.5. Sample preparation.

Cardiac tissues were homogenized in ice-cold 50 mM potassium phosphate buffer to obtain cytosolic fraction. To remove the nuclear debris, the tissue homogenate was centrifuged at 2,000 rpm for 10 minutes at 4°C and the supernatant was collected for an additional centrifugation at 14,000 rpm for 30 minutes at 4°C. The resulting supernatant was then collected as the cytosolic fraction. All the samples were stored at -20°C for subsequent biochemical analysis (32).

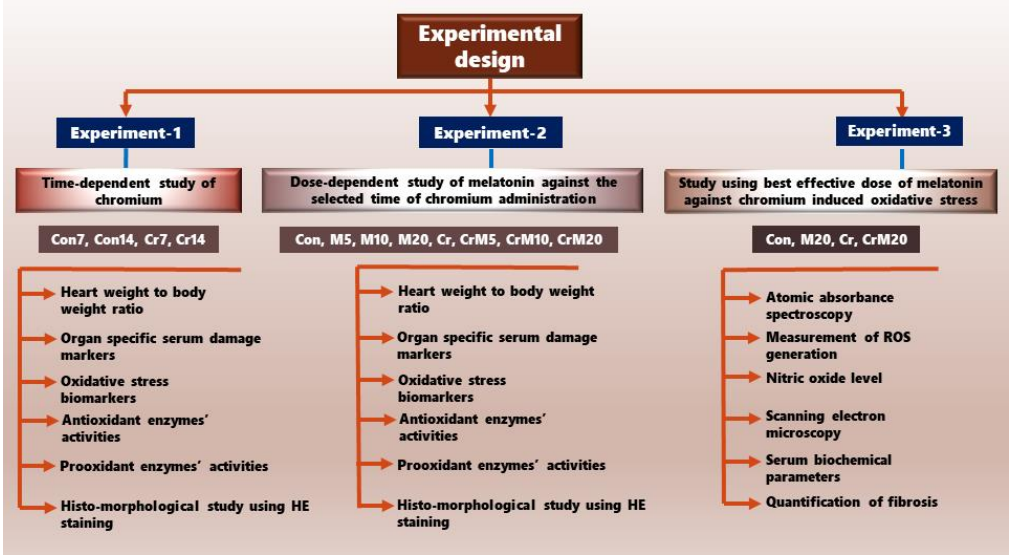

Fig. 1. Schematic representation of *in-vivo* experiments.

2.6. METHODS.

2.6.1. Determination of the ratio of heart weight to body weight.

The body weight of rats of each group was recorded at the beginning as well as at the completion of the study. After sacrifice, the heart weight was recorded carefully. Then, the ratio of heart to body weight was calculated (33).

2.6.2. Determination of the biomarkers of cardiac damage.

The activities of serum glutamate oxaloacetate transaminase (SGOT), a marker indicating cardiac tissue damage, were measured from serum using kits acquired from Arkray Healthcare Pvt. Ltd. (India). The activity measurements and computations were carried out following the instructions included with the kits. The enzyme activity was expressed in IU/L. The activity of lactate dehydrogenase-1 (LDH-1), a cardiac-specific marker was estimated using the method of Strittmatter (34) with some modifications as adopted by Varcoe (35). The activities of these enzymes were expressed in IU/L.

2.6.3. Measurements of oxidative stress biomarkers.

The levels of lipid peroxidation (LPO) in cardiac tissue homogenates were measured as thiobarbituric acid reactive substances (TBARS) using the technique of Buege and Aust (36) with minor changes made by Bandyopadhyay *et al*. (37). The absorbance was measured at 532 nm and the values were expressed as nmoles TBARS/mg of protein.

A DNPH test was used to evaluate the protein carbonyl (PCO) content in cardiac tissue homogenates (38). The results were expressed as nmoles carbonyl/mg protein.

The reduced glutathione (GSH) content of cardiac tissue homogenates was evaluated using the method of Sedlak and Lindsay (39) with some minor changes as used by Bandyopadhyay *et al.* (37). The absorbance was measured at 412 nm and expressed as nmoles GSH/mg of protein.

2.6.4. Measurements of activities of antioxidant enzymes.

The activity of superoxide dismutase (SOD) was measured from homogenates of cardiac tissues using the method established by Ewing and Janero (40). The absorbance was measured at 560 nm using a Bio-Rad microplate reader.

Catalase (CAT) activity of cardiac tissue homogenate was measured using the method of Beers and Sizer (41). The absorbance was measured at 240 nm using a UV/VIS spectrophotometer.

Glutathione peroxidase (GPx) activity was measured in the cytosolic fractions of cardiac tissues using the method of Castro *et al*. (42).

The glutathione-S-transferase (GST) activity was measured spectrophotometrically from the cytosolic fractions of the cardiac tissues following the method of Habig *et al*. (43).

The glutathione reductase (GR) activity was measured from the cytosolic fractions of the cardiac tissues by the method of Krohne-Erich *et al*. (44).

The activities of all the enzymes were expressed as U/mg protein.

2.6.5. Measurements of activities of pro-oxidant enzymes.

The activities of xanthine oxidase (XO) and xanthine dehydrogenase (XDH) in the cytosolic fractions of the cardiac tissues were measured to estimate the indirect effects of these enzymes on the production of superoxide anion *in vivo*.

The XO activity was measured spectrophotometrically at 295 nm by converting xanthine to uric acid using the method of Greenlee and Handler (45). The enzyme activity was expressed as mUnits/mg protein.

The activity of XDH was measured spectrophotometrically at 340 nm by reducing NAD^+ to NADH using the method of Strittmatter (34) with minor modifications (46). The enzyme activity was expressed as mUnits/mg protein.

2.6.6. Measurement of the activity of creatine kinase MB (CKMB).

The activity of creatine kinase MB (CKMB), a heart-specific enzyme in serum, was measured using the kits purchased from Reckon Diagnostics Pvt. Ltd. (India). All the measurements and calculations were carried out following the instructions provided with the kits. The enzyme activity was expressed in IU/L.

2.6.7. Measurement of the chromium content in the heart tissues.

The chromium content of the cardiac tissues was measured (47, 48) according to the instrument manual instructions of the "Agilent Technologies AA280" Atomic Absorption Spectrophotometer with hydride vapor generator available at the National Test House (NTH), Kolkata. The chromium content of the tissues was reported here as μg/g.

2.6.8. Cell surface architecture measurements using scanning electron microscopy (SEM).

A small portion of the heart tissue of rats from each group was preserved in 3% glutaraldehyde solution for three days and processed according to the procedure as described by Dutra *et al*. (49) with minor modifications made by Mukherjee *et al*. (50). The fixed tissues were dehydrated in graded alcohol for three days, then dehydrated again in isoamyl alcohol. Following that, the surface of the dehydrated tissue slices was examined using a SEM (Carl Zeiss).

2.6.9. Detection of reactive oxygen species (ROS) by flow cytometry.

Flow cytometry was used to detect intracellular ROS levels using a ROS marker, 2',7'-dichlorofluorescein di-acetate (DCFDA) (51), a fluorogenic dye that measures hydrogen peroxide, peroxyl, and other ROS levels. The cardiac tissue samples were treated for 30 minutes at 37º C with 2 M DCFDA dye, which is oxidized by ROS to the highly fluorescent 2',7'-dichlorofluorescein (DCF). Following incubation, all of the samples were examined using a flow cytometer (BD FACS Versa, USA) outfitted with UV filters (450-490 nm (excitation) and 520 nm (emission). FACSuite software was used to analyze the data, and the mean fluorescence intensity (MFI) was shown in a bar diagram.

2.6.10. Detection of nitric oxide (NO).

The amount of NO in the tissue samples was indirectly examined by measuring the quantities of nitrite using the Griess reagent (1% sulfanilamide and 0.1% NED in 2.5% orthophosphoric acid) and the optical density was recorded at 540 nm (52).

2.6.11. The morphological studies of cardiac tissue.

2.6.11.1. Hematoxylin-eosin (HE) staining.

A small portion of heart tissue was fixed in 10% formalin immediately for routine histological evaluation. The tissues were paraffin-embedded and 5µm thick sections were prepared. Afterward, the tissue sections were stained with hematoxylin and eosin (53). The alterations in tissue morphology were captured using a light microscope fitted with a digital camera at 20X and 40X magnifications, respectively.

2.6.11.2. Quantification of fibrosis using acid Sirius and Masson trichrome staining.

Following the usual protocol, a 5 µm section of cardiac tissue was stained with picrosirius red stain (0.1% Sirius red in saturated aqueous picric acid) for assessing the status of collagen (54). The slides were then examined and photographed using a fluorescence microscope at 20X and 40X magnifications, respectively. The photomicrographs were inspected to determine the proportion of total collagen area, which was subsequently quantified using an image processing system (Image J, NIH Software) and represented as the percent (%) collagen volume.

An additional 5 µm section was stained by Masson's trichrome stain (55–57). Freshly prepared Bouin's solution was applied to deparaffinized tissue slices and left to stand for 60 minutes. The incubated tissue slices were then rinsed with tap water to eliminate any remaining picric acid. Then, the samples were soaked with Wiegert's working hematoxylin

solution for 10 minutes, then, washed with running tap water for 5 minutes and rinsed in distilled water. After that, Biebrich scarlet solution was added to the slides and kept undisturbed for 5 minutes followed by rinsing in distilled water. Then, the slices were incubated with phosphotungstic/phosphomolybdic acid for a period of 10 minutes. Finally, aniline blue solution was applied to the slices for 5 minutes and washed in distilled water, and treated with 1% acetic acid for 1 minute. Tissue sections were then dehydrated and cleaned with xylene before being mounted with DPX. The stained tissue slices were examined using a Leica light microscope at 20X and 40X magnifications, respectively. ImageJ software was used to calculate the percentage area of fibrosis.

2.6.12. Estimation of protein.

The protein contents of cardiac tissue homogenates and cytosolic fractions were estimated following the method of Lowry et al. using BSA as standard (58).

2.7. Statistical analyses.

The data were expressed as mean ± S.E.M, and each assay was repeated at least thrice. One-way ANOVA followed by a *post-hoc* test (Tukey's HSD test) was performed to determine the significance of the mean values of different variables between different experimental groups. The results were considered statistically significant at the level of $p < 0.05$. Data were analyzed by using the IBM Statistical package for social sciences version 26 (SPSS), Microsoft Office 2019, and GraphPad prism 9.

3. RESULTS

3.1. Effects of Cr on the heart-to-body weight ratio and cardiac-specific biomarkers.

Cr treatment at day 14 significantly increased the heart-to-body-weight ratio (40.74%) compared to the control group ($p < 0.01$) (Figure 2A).

On the other hand, the activities of SGOT and LDH1 both significantly elevated on days 7 and 14, respectively in the Cr-treated groups compared to the control groups ($p< 0.01$) (Figure 2B and 2C).

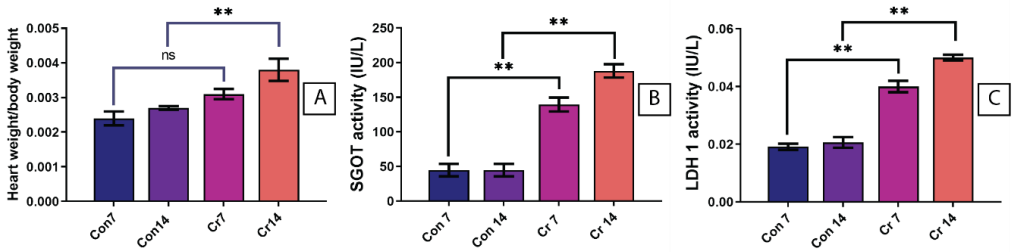

Fig. 2. Effects of Cr on the heart-to-body weight ratio and cardiac-specific biomarkers in 7 and 14 days respectively.

*(A) heart weight/body weight ratio, activities of (B) SGOT, and (C) LDH1 of rats treated with chromium. The values are expressed in mean ± SEM (n=4). Con: control, Cr: chromium, Numbers: days treated with Cr **p < 0.01.*

3.2. Effects of Cr on biomarkers of oxidative damage.

Both LPO level (1.181-fold in 7 days and 1.4-fold in 14 days) and PCO content (30.62% in 7 days and 64.57% in 14 days) were significantly increased at day 7 and 14 with Cr treatment in the cardiac tissue, respectively compared to control groups ($p< 0.01$) (Figure 3A and 3B). On the contrary, the GSH content (11.01% in 7 days and 24.01% in 14 days) was significantly decreased in the cardiac tissue of Cr treated groups, compared to controls ($p< 0.01$) (Figure 3C).

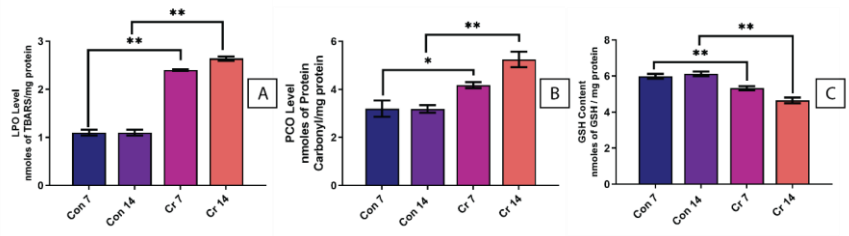

Fig. 3. Effects of Cr on oxidative stress biomarkers in cardiac tissue of rats at days 7 and 14, respectively.

*Histograms represent the levels of (A) LPO, (B) PCO, and (C) GSH. The values are expressed in mean ± SEM (n=4). C: control, Cr: chromium, Numbers: days with Cr treatment, **p < 0.01.*

3.3 Effects of Cr on the activities of antioxidant and prooxidant enzymes.

The activities of endogenous antioxidant enzymes, i.e., SOD, CAT, GST, and GR were significantly diminished both in 7 and 14 days, respectively with Cr treatment compared to control groups ($p< 0.01$) (Figure 4 A, B, D, and E). In contrast, Cr treatment significantly increased the activity of GPx in 7 and 14, respectively ($p< 0.01$) (Figure 4 C).

In the case of the activities of prooxidant enzymes in cardiac tissue, Cr treatment significantly elevated ($p<0.01$) the activities of XO, XDH, XO/XDH, XO+XDH XO/(XO+XDH) at the day 7 and 14, respectively compared to control groups (Figure 4F-J) ($p < 0.01$).

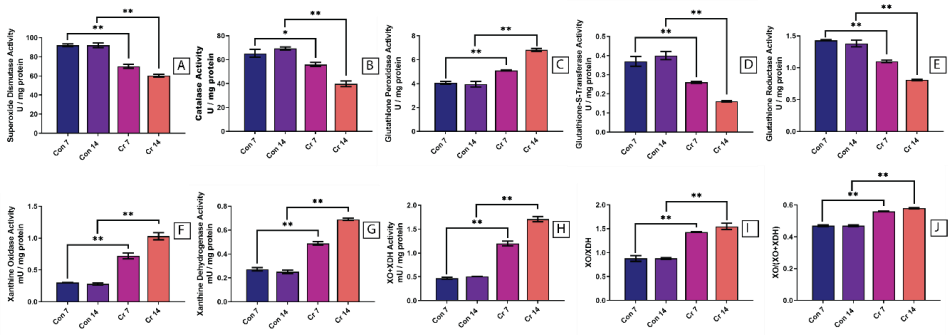

Fig. 4. Effects of Cr on the activities of endogenous antioxidant and pro-oxidant enzymes in cardiac tissue.

*Activities of antioxidant enzymes (A) SOD, (B) CAT, (C) GPX, (D) GST, and (E) GR, and pro-oxidant enzymes (F) XO, (G) XDH, (H) XO+XDH, (I) XO/XDH, (J) XO/(XO+XDH). Values are expressed as mean ± S.E.M (N = 4). Con: control, Cr: chromium, Numbers: days with Cr treatment, **p < 0.01.*

3.4. Effects of Cr on the morphological structures of cardiac tissue.

Histo-morphological studies of Cr groups of both time points exhibited severe degeneration of cardiomyocytes along with vacuolization in the cytoplasm (Figure 5 left panel). Figure 5A and 5B graphically represented the measures of ultra-structural changes in heart tissue. Cr treatment significantly reduced the total nuclear content at day 14 (Figure 5A) ($p < 0.01$), but

significantly increased the gap between consecutive fibers at day 7 and 14, respectively (Figure 5 B) ($p < 0.01$) compared to the control groups.

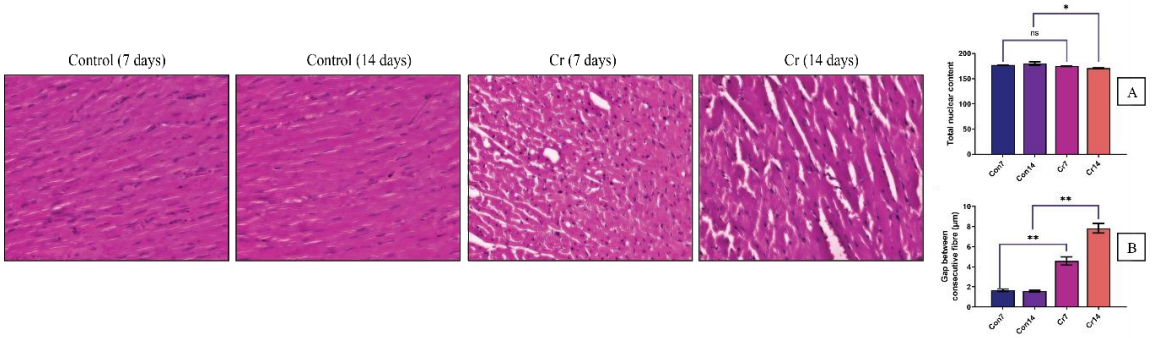

Fig. 5. Effects of Cr on histo-morphological changes in cardiac tissues.

Left panel: *photomicrographs of hematoxylin and eosin-stained cardiac tissue sections (40X magnification) which showed extensive vacuolization of cytoplasm, capillary dilatation, irregularity of myofibrils, and myocardial fiber necrosis after 7 days of treatment with a marked progression in 14 days when compared to the control rats. Fig. 5A depicts the graphical representation of total nuclear content in cardiac tissue sections of different groups. Fig. 5B represents the gap between consecutive fibres. The values are expressed in mean ± SEM). C: control, Cr: chromium, Numbers: days with Cr treatment, *p < 0.05, **p < 0.01.*

3.5. Effects of melatonin and Cr on the heart-to-body weight ratio and the activities of SGOT and LDH-1.

The results showed that Cr treatment significantly ($p < 0.01$) increased the heart-to-body weight ratio compared to the control group at day 14 while melatonin co-treatment with Cr dose-dependently reduced the increased ratio back to the control level (Figure 6 A) ($p < 0.05$ and 0.01).

Furthermore, Cr treatment significantly elevated the activities of serum SGOT and LDH-1, respectively compared to the control while these rises were significantly suppressed by melatonin co-treatment at all doses selected (Figure 6B and C) ($p < 0.01$).

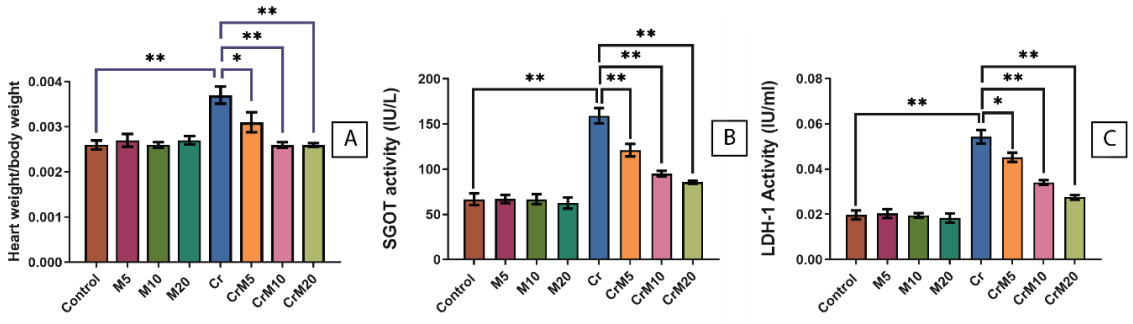

Fig. 6. Effects of Cr and melatonin on the heart-to-body weight ratio and cardiac-specific biomarkers on the day of 14.

*(A) heart weight to body weight ratio, activities of (B) SGOT, and (C) LDH1 of rats treated with chromium and melatonin at different doses. The values are expressed in mean ± SEM (n=4). Cr: chromium, M: melatonin, Numbers: melatonin doses of mg/kg., *p < 0.05, **p < 0.01.*

3.6. Effect of melatonin and Cr on oxidative stress biomarkers.

Cr treatment significantly increased the LPO and PCO levels in cardiac tissue respectively, compared to the control group while melatonin co-treatment with Cr dose-dependently suppressed these increased biomarkers (Figure 7A and B) ($p< 0.01$). On contrary, Cr treatment significantly reduced GSH content while melatonin co-treatment with Cr dose-dependently elevated this decline (Figure 7 C) ($p< 0.05$ and 0.01).

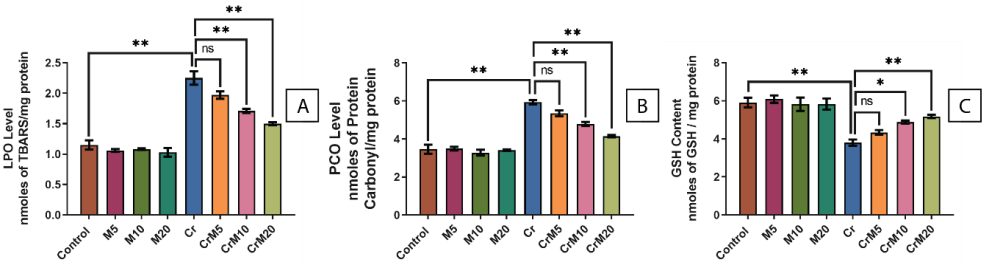

Fig. 7. Effects of melatonin and Cr on the oxidative stress biomarkers of cardiac tissue.

*The bar graph represents alterations in the levels of (A) LPO, (B) PCO, and (C) GSH content. The values are expressed in mean ± SEM (n=4). Cr: chromium, M: melatonin, Numbers: melatonin doses of mg/kg., *p < 0.05, **p < 0.01.*

3.7. Effects of melatonin and Cr on the activities of antioxidant and prooxidant enzymes of cardiac tissue.

The results showed that Cr treatment significantly reduced the activities of SOD (30.51%), CAT (49.26%), GST (60.97%), and GR (38.78%) in cardiac tissue, respectively compared to control group while melatonin co-treatment with Cr dose-dependently elevated these declines (Figure 8A, B, D and E) ($p < 0.01$). On contrary, Cr treatment significantly enhanced the GPx (49.26%) activity compared to the control group while melatonin co-treatment with Cr dose-dependently revised this increment (Figure 8C) ($P <0.01$).

On the other hand, Cr treatment significantly elevated the activities of XO (2.56-fold), XDH (1.26-fold), XO+XDH (1.77-fold), XO/XDH (57.11%), and XO/ (XO+XDH) (23.57%) of the cardiac tissue, respectively compared to control group while melatonin co-treatment with Cr dose-dependently revised these elevations significantly (Figure 8F-J) ($p<0.01$).

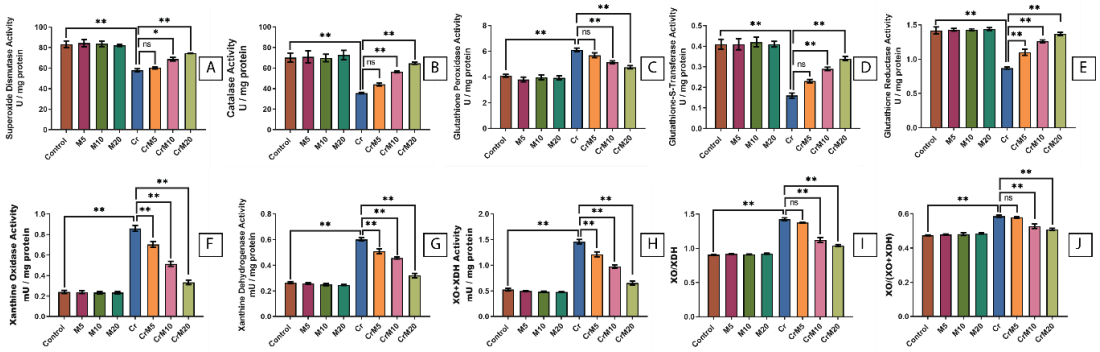

Fig. 8. Effects of melatonin and Cr on activities of antioxidant enzymes and pro-oxidant enzymes in cardiac tissue.

*(A) SOD, (B) CAT, (C) GPX, (D) GST, and (E) GR, and pro-oxidant enzymes (F) XO, (G) XDH, (H) XO+XDH, (I) XO/XDH, (J) XO/(XO+XDH). Values are expressed as mean ± S.E.M (N = 4). Cr: chromium, M: melatonin, Numbers: melatonin doses of mg/kg., *p < 0.05, **p < 0.01.*

3.8. Effects of melatonin and Cr on the morphological structure of cardiac tissue.

Profound morphological damages including degeneration, vacuolization, and congestion were found in the cardiac tissue of the Cr-treated group compared to the control group while melatonin co-treatment with Cr dose-dependently prevented these damages (Figure 9 left panels). The statistical analyses confirmed the morphological observations. The Cr treatment significantly reduced the total nuclear content (2.49%) and the gap between consecutive fibers (3.04-fold) of the cardiac tissue compared to the control group while melatonin co-treatment with Cr dose-dependently minimized these alterations (Figure 9A and B) ($p < 0.05$ or 0.01).

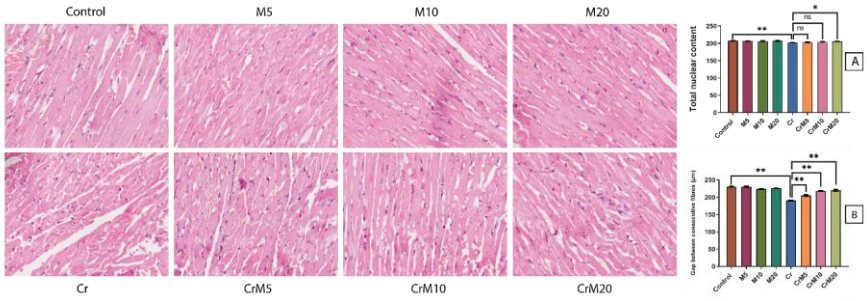

Fig. 9. Effects of melatonin and Cr on histo-morphological changes in cardiac tissues.

*The left panels were the photomicrographs of hematoxylin eosin-stained cardiac tissue sections (40X magnification) representing all the structural alterations (discussed previously in Fig.5) (A) The statistical analysis of total nuclear content. (B) The gaps between fibers. Cr: chromium, M: melatonin, Numbers: melatonin doses of mg/kg., *p < 0.05, **p < 0.01.*

3.9. Effects of melatonin and Cr on the deposition of chromium, ROS, and NO generation in cardiac tissue.

The results showed that Cr treatment significantly increased the Cr content (56.80%) (Figure 10 A) and ROS production (55.29%) (Figure 10 C) of cardiac tissue, respectively compared to the control group while melatonin co-treatment with Cr at the dose of 20 mg/kg reduced these increases back to the control levels (Figure 10A and B) ($p < 0.01$). In contrast, Cr treatment significantly reduced the NO level (61.11%) of cardiac tissue compared to the control group, however, melatonin co-treatment with Cr at the dose of 20 mg/kg significantly reduced this decline (Figure 10D) ($p < 0.01$).

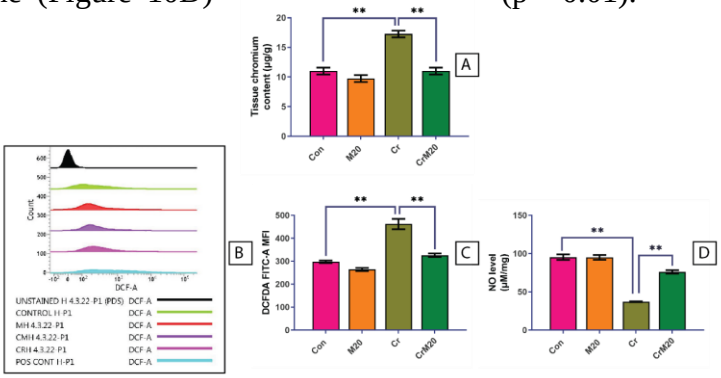

Fig. 10. Effects of melatonin on Cr concentration in cardiac tissue and its impact on ROS and NO generation.

*(A) Cr concentration, (B) offset layout representation of DCFDA, (C) mean fluorescence intensity (MFI) of DCFDA FITC-A which represents the intracellular ROS levels, and (D) NO level in the cardiac tissue. The values are expressed in Mean ± SEM. Cr: chromium, M: melatonin, Numbers: melatonin dose of mg/kg., **p < 0.01.*

3.10. Effects of melatonin and Cr on the surface topology of cardiac tissue and serum CK-MB activity.

SEM was used to evaluate architectural changes in cardiac tissue. In the Cr-treated group, under 5KX magnification, abnormal distribution and breakage of cardiac muscle fibers were noticed due to the formation of a complicated matrix network along with creases and uneven surfaces of the endocardium compared to the control while melatonin co-treatment with Cr at the dose of 20 mg/kg normalized these alterations (Figure 11, left panels).

The activity of CK-MB (Fig.11A) was significantly increased in the Cr-treated group (1.38-fold) compared to the control group while melatonin co-treatment with Cr at the dose of 20mg/kg suppressed this increase significantly (Figure 11A).

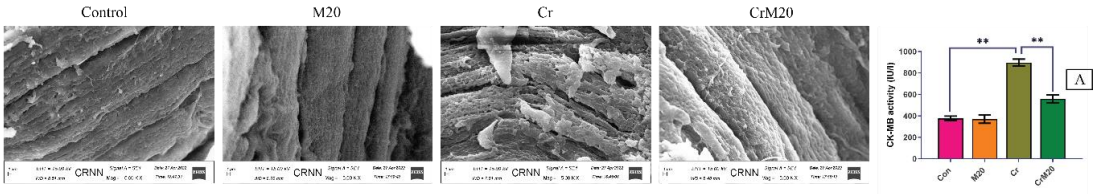

Fig. 11. Effects of melatonin and Cr on the surface architecture of cardiac tissue and level of CK-MB.

The left panels were *representative SEM images depicting the surface architecture of cardiac tissue sections. The furrowing and necrosis due to the degeneration of cardiac tissue induced by Cr were observed. Whereas, the control group and melatonin-treated group showed normal texture and regularities of myofibrils. (A) CK-MB level. Cr: chromium, M: melatonin, Numbers: melatonin dose of mg/kg., **p < 0.01.*

3.11. Effects of melatonin and Cr on collagen content in cardiac tissue.

The collagen content of cardiac tissue was measured by two staining procedures, i.e., picrosirius red staining by fluorescence microscopy and Masson trichrome staining through brightfield microscopy respectively (Figure 12 left panels). Both staining procedures revealed that Cr treatment caused the deposition of collagen fibers between the muscle fibers of heart tissue thus projecting fibrosis. Melatonin co-treatment with Cr suppressed collagen deposition and fibrosis. The statistical analyses also confirmed the above observations, i.e., collagen contents measured by both staining's were significantly increased in the Cr-treated compared to the control group; however, melatonin co-treatment with CR at the dose of 20 mg/kg reversed this increase back to control level (Figure 12A and B).

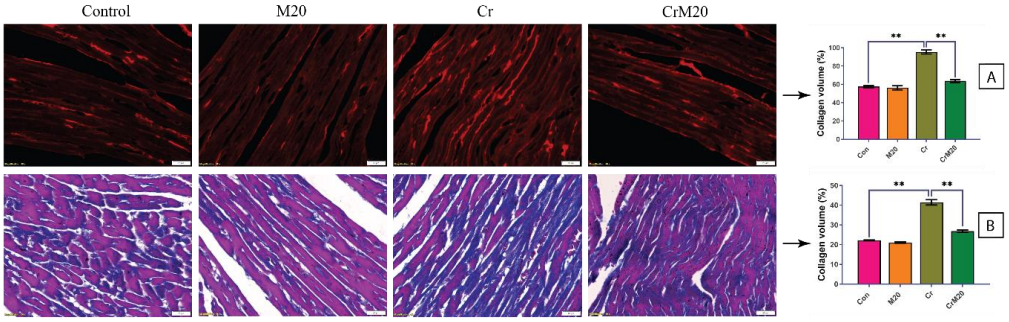

Fig. 12. Effects of melatonin and Cr on collagen content of cardiac tissue.

The left panels are representatives of photomicrographs (20X magnification) of collagen content in cardiac tissue measured by acid-Sirius red (up) and Masson trichrome (low) staining's red and blue colours were the areas of collagen. (A) collagen volume (%)

*measured by acid-Sirius red staining, (B) collagen volume (%) measured by Masson trichrome staining. Cr: chromium, M: melatonin, Numbers: melatonin dose of mg/kg., **p < 0.01.*

4. DISCUSSION

Environmental pollution is considered a potential risk factor for CVD and its health threat has drowned the global concern currently (59). For example, a growing number of individuals are exposed to Cr from various industry sources, polluted foods, and water (60). This exposure will increase the prevalence of CVD. Mechanistically, Cr exposure causes excessive production of free radicals which leads to disruption of cellular redox status, protein and lipid oxidation as well as reduced activities of both enzymatic and non-enzymatic antioxidants (61). These alterations interrupt cellular defense mechanisms and inevitably result in the pathogenesis of cardiac tissue (62). It seems that antioxidants may protect the Cr-caused cardiac injury by targeting free radicals and oxidative stress. Melatonin is an endogenously occurring antioxidant. Therefore, in the current study, we tested the potential therapeutic effects of melatonin on Cr-induced cardiac damage.

First, we established the Cr pathological animal model by giving rats Cr at a dosage of 5 mg/kg for 14 days. It was found that this treatment caused maximum cardiac damage assessed by the histological and biochemical parameters but avoided mortality during the entire treatment period. The results were consistent with the previous report (31). Then, the protective effects of melatonin were tested. The results showed that all the doses of melatonin tested in the study counteracted the harmful effects of Cr in experimental rats. Among the doses, 20mg/kg/day of melatonin was the best effective dose for treating Cr-induced infirmities.

The Cr treatment caused a significant rise in the ratio of heart to body weight. This may be due to Cr being absorbed and accumulated in the heart tissue (63, 64), which also contributes to the development of cardiac injury. This raised ratio is minimized by melatonin in a dose-dependent manner. Melatonin can chelate heavy metals thus, it may chelate both Cr (VI) and Cr (III) before they are absorbed by tissues and therefore, reduces the Cr load in cardiac tissue

The Cr also caused increases in the activities of SGOT and LDH1 indicating substantial damage to cardiac tissue. This was confirmed by the abnormal ultra-structural changes including myonecrosis, vacuolization, hemorrhage, and fibrosis in cardiac tissue after Cr treatment (65). The increased activity of these cardiac enzymes also suggested increased cellular permeability and the compromise of membrane architectural and functional integrity (66). These alterations were protected by melatonin co-treatment via preserving membrane integrity (67, 68). This is attributed to melatonin scavenging a wide range of ROS while also boosting the activities of antioxidant enzymes (24), therefore, inhibiting oxidative stress.

The LPO and PCO formations are indicators of tissue oxidative stress. Cr promoted their formations (69). For example, the metabolites of Cr interact with H_2O_2 and superoxide anion to produce more dangerous free radicals to subtract a hydrogen atom from a methylene group of polyunsaturated fatty acids, elevating LPO (70) and PCO (71). Some theories have been put forth to explain how Cr (VI) is metabolized to Cr (III) in the extracellular environment. Cr (III) is membrane impermeable and accumulated inside of the cell to readily cause lipids and protein damage and loss of cellular as well as morphological integrity (72). To defend against oxidative stress, glutathione plays a vital role in maintaining the redox state of cells. The thiol (-SH) group of glutathione chelates the metal ions to neutralize them (73). The highly-affine thiol group of GSH may bind to chromium to detoxify it. In addition, GSH scavenges free radicals generated by chromium (65, 74) and reduces Cr (VI) into its various

metabolites in the intracellular environment (75, 76). In the current study, it was found that Cr significantly reduced the GSH content; however, melatonin co-treatment dose-dependently recovered the GSH content with the reduction of LPO and PCO levels. Since the cell membrane is the prime site of lipid peroxidation and protein oxidation the results indicated melatonin plays a pivotal role in protecting the cell membrane (13, 77), defending the membrane against lipophilic-oxy radicals and hydrophilic radicals that occur in an aqueous environment (78). The protective effects of melatonin on lipid peroxidation (79) and protein oxidation (80) have been well documented. The metal-chelating activity of melatonin (81) can also thermodynamically interacts with GSH and inhibits it to bind to metals and thus, replenishing GSH (82) from Cr toxicity.

It is also found that the activities of antioxidant enzymes including SOD, CAT, GPX, GST, and GR were altered by Cr treatment. For example, the decreased SOD and CAT with a concurrent rise in GPX activity were identified in the cardiac tissue. Decreased CAT activity can elevate H_2O_2 and the reduced SOD activity can generate a surplus of superoxide anion in heart tissue. It has been reported that increases in the activities of SOD and CAT decrease DNA single-strand breaks induced by Cr (VI) (83). A decline in the level of GSH in heart tissue after Cr treatment is also linked to an increase in GPX activity observed in the study. However, the decrease in CAT activity caused by Cr has been associated with the structural modification of this enzyme as seen in other enzymes (84). GST plays a key role in covalent binding to reactive electrophiles by increasing the oxidation of GSH (85). The reduced GST activity may also result from the drop in GSH content under the influence of Cr (60). A decrease in GR activity is strongly associated with Cr (VI) metabolism and the generation of harmful intermediates. Cr (VI) binds to NADPH to form the Cr-(V)-NADPH complex, which inhibits GR action and causes DNA damage (86). The protective effects of melatonin on Cr-induced damages in all these antioxidant enzymes are majorly attributed to its direct free radical detoxification (87). Melatonin can effectively quench singlet oxygen ($^1O_2$) (88), peroxyl radical (ROO·) (89), hypochlorous acid (HOCl) (90), HO· (91), H_2O_2, $O_2^{\cdot-}$ (92), and others. Moreover, it stimulates the expression of several antioxidant enzymes such as SOD, CAT, GPx, and GR (25, 93–95).

XO and XDH are single-gene products that utilize the same precursor, either xanthine or hypoxanthine, but generate distinct products utilizing separate co-factors. $O^{2.-}$ is formed by both processes, but XO uses O_2 as a co-factor to produce uric acid, whereas XDH uses NAD to produce NADH. XO is the principal producer of oxygen radicals that regulate cellular oxidative balance (96). The current study showed that Cr treatment promoted the production of $O^{2.-}$, which was projected by the increased XO and XDH activities as well as the ratios of XO/XDH, XO+XDH, and XO/ (XO + XDH) in the cardiac tissue. Remarkably, melatonin therapy lowered pro-oxidant enzyme activity to the baseline levels, most likely by neutralizing free radicals.

Histological examinations provided additional support for all the alterations caused by Cr mentioned above. HE staining identified considerable morphological alterations including myofibril degeneration, necrosis, and vacuolization in Cr-treated animals (74). The findings from HE staining were further confirmed by the SEM investigation which also revealed considerable morphological degeneration in cardiac tissues after Cr treatment. Again, melatonin co-treatment significantly restored all Cr-induced histo-morphological abnormalities by its antioxidant activity

From the point of view of pharmacokinetics, the half-life of Cr in tissue is typically 39 hours (97). Banerjee *et al*. have also reported that the maximum accumulation of Cr in tissues is within 15 days, but it then remains for a very long time (87). The primary way to excrete Cr from the body is through urine. The kidney excretes about 60% of Cr within 8 hours after

its intake (98). Pre-treatment with melatonin reduced the Cr accumulation due to its chelating activity to heavy metals (99) and this was observed in the current study.

CK-MB can be used to diagnose myocardial damage induced by Cr (100). CK-MB is released from the cytosol into the systemic circulation due to cell membrane disruption (101). Thus, increased CK-MB activity after Cr treatment indicates lipid and protein oxidation-linked cell membrane damage. Co-treatment with melatonin restored the activities of CK-MB, presumably by conserving membrane integrity with its antioxidant properties.

In addition to ROS, Cr can also promote reactive nitrogen species formation. Cr (VI) is in the transitional state, it can cause nitrosative stress by producing nitric oxide (20) and peroxynitrite (ONOO-). Cr (VI) stimulates the synthesis of $O_2^{\cdot-}$ which rapidly interacts with NO and forms hazardous ONOO- and causes tissue damage (102). Furthermore, NOS may convert Cr(VI) to Cr(V) in a single step (103) to generate more toxic intermediates. In this respect, melatonin inhibits NOS (104) to prevent NOS from converting Cr(VI) to Cr(V), protecting the tissue from its toxic residues while also maintaining the average cellular level of NO and boosting its bioavailability (105).

Finally, Cr caused cardiac tissue with significant collagen build-up detected by picrosirius and Masson-trichrome staining, indicating fibrosis and chronic inflammation of cardiac tissue (106). However, melatonin co-administration prevented such deleterious repercussions of Cr on cardiac tissue.

Therefore, all evidence showed the adverse effects of Cr exposure on heart health and the protective potential of melatonin on Cr cardiac toxicity. These were summarized in Figure 13.

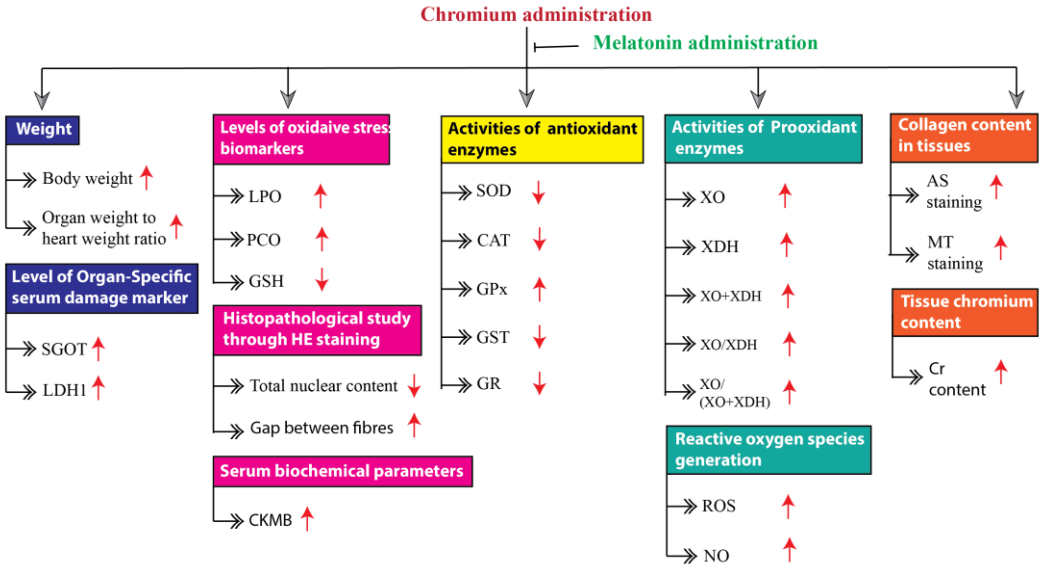

Fig. 13. Summarization of the pathological effects of Cr on cardiac tissue and the protection of melatonin on them.

5. CONCLUSION

The results of the current study confirmed that Cr promoted the formation of ROS/RNS which caused oxidative cardiac damage including necrosis and fibrosis in rats. On the other hand, melatonin co-treatment provided strong protection against Cr-induced undesirable cardiac physiopathological alterations mediated by oxidative stress. The mechanism of action of melatonin may include scavenging ROS/RNS or accelerating their decomposition via upregulating a spectrum of antioxidant enzymes. Melatonin is a naturally occurring

antioxidant with minimal side effects or toxicity. It is essentially available in all foods in various amounts, therefore incorporating it into a person's daily routine as a bio-protectant or bio-remediation. Thus, melatonin may be a novel approach for treating oxidative stress-induced cardiovascular disease in humans.

ACKNOWLEDGMENTS

PG gratefully acknowledges the receipt of the Senior Research Fellowship [1571/) PWD NET-NOV2017]. TD was UGC-SRF [No.F.15-9(JUNE 2015)/2015(NET)] under UGC, Govt. of India. Prof. DB is supported by the funds available from the Teacher's Research Grant (BI grant) of University of Calcutta. The authors thankfully acknowledge the technical help of Dr. Sneha Mitra and Pratyush Sengupta, Center of Excellence for Nanobiotechnology (CRNN), University of Calcutta, for the Flowcytometric studies and SEM studies. The authors are grateful to Department of Physiology Govt. Of India for brightfield microscopy. The authors are grateful to the National Test House for allowing them to utilize their facility to perform the AAS experiment.

AUTHORSHIP

Dr. DB and Dr. AC conceived and designed the experiment, revised the manuscript critically, and approved it. PG executed the experiment, analysed the data, prepared figures, drafted the manuscript, and edited it. MD and TD contributed to executing the experiments. RM helped in the analysis of tissue morphology.

CONFLICTS OF INTEREST

The authors have no conflict of interest.

ABBREVIATIONS

$O_2^{\cdot-}$: Superoxide anion radical
CAT: Catalase
Cr: Chromium
Cr (III): Trivalent chromium
Cr (VI): Hexavalent chromium
GPx: Glutathione peroxidase
GSH: Reduced glutathione
GSSG: Oxidized glutathione
H_2O_2: Hydrogen peroxide
$HO^{\cdot}$: Hydroxyl radical
LPO: Lipid peroxidation
NAD+: Nicotinamide adenine dinucleotide (oxidized)
NADH: Nicotinamide adenine dinucleotide (reduced)
NADPH: Nicotinamide adenine dinucleotide phosphate
ONOO-: Peroxynitrite
RNS: Reactive nitrogen species
ROS: Reactive oxygen species
FITC: Fluorescein isothiocyanate
FACS: Fluorescence-activated cell sorting
nm: nanometer

μM: Micro mole
SEM: Standard error of the mean
BSA: Bovine serum albumin
DNA: Deoxyribonucleic acid
DNPH: Dinitrophenyl hydrazine

REFERENCES

1. Benjamin EJ, Muntner P, Alonso A, Bittencourt MS, Callaway CW, Carson AP *et al.* (2019) Heart Disease and Stroke Statistics-2019 Update: A Report From the American Heart Association. *Circulation* **139** (10): e56–e528. DOI: 10.1161/CIR.0000000000000659.
2. Cosselman KE, Navas-Acien A, Kaufman JD (2015) Environmental factors in cardiovascular disease. *Nat. Rev. Cardiol.* **12** (11): 627–642. DOI: 10.1038/nrcardio.2015.152.
3. Ali H, Khan E, Ilahi I (2019) Environmental chemistry and ecotoxicology of hazardous heavy metals: environmental persistence, toxicity, and bioaccumulation. *J. Chem.* **2019** : 1–14. DOI: 10.1155/2019/6730305.
4. Tchounwou PB, Yedjou CG, Patlolla AK, Sutton DJ (2012) Molecular, clinical and environmental toxicology. Luch A, editor. Molecular, Clinical and Environmental Toxicology. Basel: Springer Basel; **2012**: 133–164 p. (Experientia Supplementum; vol. 101). DOI: 10.1007/978-3-7643-8340-4.
5. Zhang XH, Zhang X, Wang XC, Jin LF, Yang ZP, Jiang CX, Chen Q, Ren X Bin, Cao JZ, Wang Q, Zhu YM (2011) Chronic occupational exposure to hexavalent chromium causes DNA damage in electroplating workers. *BMC Public Health*. **11** (224): 1–8. DOI: 10.1186/1471-2458-11-224.
6. Becerra-Torres SL, Rodríguez-Vázquez ML, Medina-Ramírez IE, Jaramillo-Juárez F (2009) The flavonoid quercetin protects and prevents against potassium dichromate–induced systemic peroxidation of lipids and diminution in renal clearance of para-aminohippuric acid and inulin in the rat. *Drug Chem. Toxicol.* **32** (1): 88–91. DOI: 10.1080/01480540802449951.
7. Rajeev P, Rajput P, Singh DK, Singh AK, Gupta T (2018) Risk assessment of submicron PM-bound hexavalent chromium during wintertime. *Hum. Ecol. Risk Assess. An Int. J.* **24** (6): 1453–1463. DOI: 10.1080/10807039.2017.1414581.
8. Coyte RM, McKinley KL, Jiang S, Karr J, Dwyer GS, Keyworth AJ, Davis CC, Kondash AJ, Vengosh A (2020) Occurrence and distribution of hexavalent chromium in groundwater from North Carolina, USA. *Sci. Total Environ.* **711** (135135): 1–40. DOI: 10.1016/j.scitotenv.2019.135135.
9. Chromium Global Market Review 2022 and Forecast to 2031.
10. Mishra S, Bharagava RN (2016) Toxic and genotoxic effects of hexavalent chromium in environment and its bioremediation strategies. *J. Environ. Sci. Heal. - Part C Environ. Carcinog. Ecotoxicol. Rev.* **34** (1): 1–32. DOI: 10.1080/10590501.2015.1096883.
11. Sharma P, Singh SP, Parakh SK, Tong YW (2022) Health hazards of hexavalent chromium (Cr (VI)) and its microbial reduction. *Bioengineered* **13** (3): 4923–4938. DOI: 10.1080/21655979.2022.2037273.
12. von Burg R, Liu D (1993) Chromium and hexavalent chromium. *J. Appl. Toxicol.* **13** (3): 225–230. DOI: 10.1002/jat.2550130315.
13. Costa EJX, Shida CS, Biaggi MH, Ito AS, Lamy-Freund MT (1997) How melatonin interacts with lipid bilayers: A study by fluorescence and ESR spectroscopies. *FEBS Lett.* **416** (1): 103–106. DOI: 10.1016/S0014-5793(97)01178-2.

14. Costa M (1997) Toxicity and carcinogenicity of Cr(VI) in animal models and humans. *Crit. Rev. Toxicol.* **27** (5): 431–442. DOI: 10.3109/10408449709078442.
15. Shi X, Dalal NS (1990) On the hydroxyl radical formation in the reaction between hydrogen peroxide and biologically generated chromium(V) species. *Arch. Biochem. Biophys.* **277** (2): 342–350. DOI: 10.1016/0003-9861(90)90589-Q.
16. Sharma B, Singh S, Siddiqi NJ (2014) Biomedical implications of heavy metals induced imbalances in redox systems. *Biomed Res. Int.* **2014** (640754): 1–26. DOI: 10.1155/2014/640754.
17. Stohs SJ, Bagchi D (1995) Oxidative mechanisms in the toxicity of metal ions. *Free Radic. Biol. Med.* **18** (2): 321–336. DOI: 10.1016/0891-5849(94)00159-H.
18. Ghosh P, Dey T, Chattopadhyay A, Bandyopadhyay D (2021) An insight into the ameliorative effects of melatonin against chromium induced oxidative stress and DNA damage: a review. *Melatonin Res.* **4** (3): 377–407. DOI: 10.32794/MR112500101.
19. Nuran Ercal BSP, Hande Gurer-Orhan BSP, Nukhet Aykin-Burns BSP (2001) Toxic metals and oxidative stress part I: mechanisms involved in metal induced oxidative damage. *Curr. Top. Med. Chem.* **1** (6): 529–539. DOI: 10.2174/1568026013394831.
20. Valko M, Morris H, Cronin M (2005) Metals, toxicity and oxidative stress. *Curr. Med. Chem.* **12** (10): 1161–1208. DOI: 10.2174/0929867053764635.
21. Qi W, Reiter RJ, Tan DX, Garcia JJ, Manchester LC, Karbownik M, Calvo JR (2000) Chromium(III)-induced 8-hydroxydeoxyguanosine in DNA and its reduction by antioxidants: Comparative effects of melatonin, ascorbate, and vitamin E. *Environ. Health Perspect.* **108** (5): 399–403. DOI: 10.1289/ehp.00108399.
22. Xin Z, Zhang X, Hu W, Tan DX, Han M, Ji T, Jiang S, Yu Z, Reiter RJ, Yang Y (2019) The protective effects of melatonin on organisms against the environmental pollutants of heavy metal and non-mental toxins. *Melatonin Res.* **2** (4): 99–120. DOI: 10.32794/11250043.
23. Dominguez-Rodriguez A, Abreu-Gonzalez P, Sanchez-Sanchez JJ, Kaski JC, Reiter RJ (2010) Melatonin and circadian biology in human cardiovascular disease. *J. Pineal Res.* **49** (1): 1-10. DOI: 10.1111/j.1600-079X.2010.00773.x.
24. Reiter RJ, Mayo JC, Tan D-X, Sainz RM, Alatorre-Jimenez M, Qin L (2016) Melatonin as an antioxidant: under promises but over delivers. *J. Pineal Res.* **61** (3): 253–278. DOI: 10.1111/jpi.12360.
25. Rodriguez C, Mayo JC, Sainz RM, Antolín I, Herrera F, Martín V, Reiter RJ (2004) Regulation of antioxidant enzymes: A significant role for melatonin. *J. Pineal Res.* **36** (1): 1–9. DOI: 10.1046/j.1600-079X.2003.00092.x.
26. Tan D-X, Manchester LC, Hardeland R, Lopez-Burillo S, Mayo JC, Sainz RM, Reiter RJ (2003) Melatonin: a hormone, a tissue factor, an autocoid, a paracoid, and an antioxidant vitamin. *J. Pineal Res.* **34** (1): 75–78. DOI: 10.1034/j.1600-079X.2003.02111.x.
27. Acuña-Castroviejo D, Escames G, Venegas C, Díaz-Casado ME, Lima-Cabello E, López LC, Rosales-Corral S, Tan DX, Reiter RJ (2014) Extrapineal melatonin: Sources, regulation, and potential functions. *Cell. Mol. Life Sci.* **71** (16): 2997–3025. DOI: 10.1007/S00018-014-1579-2/FIGURES/4.
28. Cheng G, Ma T, Deng Z, Gutiérrez-Gamboa G, Ge Q, Xu P, Zhang Q, Zhang J, Meng J, Reiter RJ, Fang Y, Sun X (2021) Plant-derived melatonin from food: a gift of nature. *Food Funct.* **12** (7): 2829–2849. DOI: 10.1039/D0FO03213A.
29. Meng X, Li Y, Li S, Zhou Y, Gan R-Y, Xu D-P, Li H-B (2017) Dietary sources and bioactivities of melatonin. *Nutrients* **9** (4): 367. DOI: 10.3390/nu9040367.
30. A Hattori, H Migitaka, M Iigo, M Itoh, K Yamamoto, R Ohtani-Kaneko, M Hara, T Suzuki RJR (1985) Identification of melatonin in plants and its effects on plasma melatonin levels and binding to melatonin receptors in vertebrates. *Biochem. Mol. Biol.*

Int. **35** (3): 627–634.
31. Kim E, Na KJ (1991) Nephrotoxicity of sodium dichromate depending on the route of administration. *Arch. Toxicol.* **65** (7): 537–541. DOI: 10.1007/BF01973713.
32. Mukherjee D, Roy SG, Bandyopadhyay A, Chattopadhyay A, Basu A, Mitra E, Ghosh AK, Reiter RJ, Bandyopadhyay D (2010) Melatonin protects against isoproterenol-induced myocardial injury in the rat: antioxidative mechanisms. *J. Pineal Res.* **48** (3): 251–262. DOI: 10.1111/j.1600-079X.2010.00749.x.
33. Dey T, Ghosh A, Mishra S, Pal PK, Chattopadhyay A, Pattari SK, Bandyopadhyay D (2020) Attenuation of arsenic induced high fat diet exacerbated oxidative stress mediated hepatic and cardiac injuries in male Wistar rats by piperine involved antioxidative mechanisms. *Food Chem. Toxicol.* **142** (111477): 1–87. DOI: 10.1016/j.fct.2020.111477.
34. Strittmatter CF (1965) Studies on Avian Xanthine Dehydrogenases. Properties and Patterns of Appearance During Development. *J. Biol. Chem.* **240** (6): 2557–2564. DOI: 10.1016/S0021-9258(18)97361-8.
35. Varcoe JS (2001) Clinical biochemistry: techniques and instrumentation. World Scientific. WORLD SCIENTIFIC; 2001. DOI: 10.1142/4635.
36. Buege JA, Aust SD (1978) Microsomal lipid peroxidation. In: Journal of Physics: Conference Series. 1978. p. 302–310. DOI: 10.1016/S0076-6879(78)52032-6.
37. Bandyopadhyay D, Ghosh G, Bandyopadhyay A, Reiter RJ (2004) Melatonin protects against piroxicam-induced gastric ulceration. *J. Pineal Res.* **36** (3): 195–203. DOI: 10.1111/j.1600-079X.2004.00118.x.
38. Levine RL, Williams JA, Stadtman EP, Shacter E (1994) Carbonyl assays for determination of oxidatively modified proteins. In: Methods in Enzymology. Methods Enzymol; 1994. p. 346–357. DOI: 10.1016/S0076-6879(94)33040-9.
39. Sedlak J, Lindsay RH (1968) Estimation of total, protein-bound, and nonprotein sulfhydryl groups in tissue with Ellman's reagent. *Anal. Biochem.* **25** (1): 192–205. DOI: 10.1016/0003-2697(68)90092-4.
40. Ewing JF, Janero DR (1995) Microplate superoxide dismutase assay employing a nonenzymatic superoxide generator. *Anal. Biochem.* **232** (2): 243–248. DOI: 10.1006/abio.1995.0014.
41. Beers RF, Sizer IW (1952) A sprectrophotometric method for measuring the breakdown of hydrogen peroxide by catalase. *J. Biol. Chem.* **195** (1): 133–140. DOI: 10.1016/S0021-9258(19)50881-X.
42. Castro R, Piazzon MC, Noya M, Leiro JM, Lamas J (2008) Isolation and molecular cloning of a fish myeloperoxidase. *Mol. Immunol.* **45** (2): 428–437. DOI: 10.1016/j.molimm.2007.05.028.
43. Habig WH, Pabst MJ, Jakoby WB (1974) Glutathione S-Transferases. *J. Biol. Chem.* **249** (22): 7130–7139. DOI: 10.1016/S0021-9258(19)42083-8.
44. Krohne-Ehrich G, Schirmer RH, Untucht-Grau R (1977) Glutathione reductase from human erythrocytes. isolation of the enzyme and sequence analysis of the redox-active peptide. *Eur. J. Biochem.* **80** (1): 65–71. DOI: 10.1111/j.1432-1033.1977.tb11856.x.
45. Greenlee L, Handler P (1964) Xanthine oxidase. *J. Biol. Chem.* **239** (4): 1090–1095. DOI: 10.1016/S0021-9258(18)91395-5.
46. Mitra E, Ghosh AK, Ghosh D, Mukherjee D, Chattopadhyay A, Dutta S, Pattari SK, Bandyopadhyay D (2012) Protective effect of aqueous Curry leaf (Murraya koenigii) extract against cadmium-induced oxidative stress in rat heart. *Food Chem. Toxicol.* **50** (5): 1340–1353. DOI: 10.1016/j.fct.2012.01.048.
47. Hilliard EP, Smith JD (1979) Minimum sample preparation for the determination of ten elements in pig faeces and feeds by atomic-absorption spectrophotometry and a spectrophotometric procedure for total phosphorus. *Analyst* **104** (1237): 313. DOI:

10.1039/an9790400313.
48. Capar SG, Tanner JT, Friedman MH, Boyer KW (1978) Multielement analysis of animal feed, animal wastes, and sewage sludge. *Environ. Sci. Technol.* **12** (7): 785–790. DOI: 10.1021/es60143a004.
49. Noronha Dutra AA, Steen EM, Woolf N (1984) The early changes induced by isoproterenol in the endocardium and adjacent myocardium. *Am. J. Pathol.* **114** (2): 231.
50. Mukherjee D, Ghosh AK, Bandyopadhyay A, Basu A, Datta S, Pattari SK, Reiter RJ, Bandyopadhyay D (2012) Melatonin protects against isoproterenol-induced alterations in cardiac mitochondrial energy-metabolizing enzymes, apoptotic proteins, and assists in complete recovery from myocardial injury in rats. *J. Pineal Res.* **53** (2): 166–179. DOI: 10.1111/j.1600-079X.2012.00984.x.
51. Bhogal RH, Curbishley SM, Weston CJ, Adams DH, Afford SC (2010) Reactive oxygen species mediate human hepatocyte injury during hypoxia/reoxygenation. *Liver Transpl.* **16** (11): 1303–1313. DOI: 10.1002/LT.22157.
52. Green LC, Wagner DA, Glogowski J, Skipper PL, Wishnok JS, Tannenbaum SR (1982) Analysis of nitrate, nitrite, and [15N]nitrate in biological fluids. *Anal. Biochem.* **126** (1): 131–138. DOI: 10.1016/0003-2697(82)90118-X.
53. Suvarna K, Layton C, Bancroft J (2018) Bancroft's theory and practice of histological techniques E-Book. 2018.
54. Junqueira LCU, Bignolas G, Brentani RR (1979) Picrosirius staining plus polarization microscopy, a specific method for collagen detection in tissue sections. *Histochem. J.* **11** (4): 447–455. DOI: 10.1007/BF01002772.
55. Sheehan DC, Hrapchak BB 1987. 2. ed. (1987) Theory and practice of histotechnology. Columbus Ohio: Battelle Press; 1987. 481 p.
56. Bancroft J, Gamble M (2008) Theory and practice of histological techniques.
57. Luna L (1968) Manual of histologic staining methods of the Armed Forces Institute of Pathology. McGrow-Hill, NY.
58. Lowry OH, Rosebrough NJ, Farr AL, Randall RJ (1951) Protein measurement with the Folin phenol reagent. *J. Biol. Chem.* **193** (1): 265–275. DOI: 10.1016/s0021-9258(19)52451-6.
59. Yang A, Lo K, Zheng T, Yang J, Bai Y, Feng Y, Cheng N, Liu S (2020) Environmental heavy metals and cardiovascular diseases: Status and future direction. *Chronic Dis. Transl. Med.* **6** (4): 251–259. DOI: 10.1016/j.cdtm.2020.02.005.
60. Sahu BD, Koneru M, Bijargi SR, Kota A, Sistla R (2014) Chromium-induced nephrotoxicity and ameliorative effect of carvedilol in rats: Involvement of oxidative stress, apoptosis and inflammation. *Chem. Biol. Interact.* **223** (2014): 69–79. DOI: 10.1016/j.cbi.2014.09.009.
61. Ahmad MK, Syma S, Mahmood R (2011) Cr(VI) induces lipid peroxidation, protein oxidation and alters the activities of antioxidant enzymes in human erythrocytes. *Biol. Trace Elem. Res.* **144** (1–3): 426–435. DOI: 10.1007/s12011-011-9119-5.
62. Barhoma RAE (2018) The role of eugenol in the prevention of chromium-induced acute kidney injury in male albino rats. *Alexandria J. Med.* **54** (4): 711–715. DOI: 10.1016/j.ajme.2018.05.006.
63. Lopotych N, Panas N, Datsko T, Slobodian S (2020) Influence of heavy metals on hematologic parameters, body weight gain and organ weight in rats. *Ukr. J. Ecol.* **10** (1): 175–179. DOI: 10.15421/2020_28.
64. Honda K, Sahrul M, Hidaka H, Tatsukawa R (1983) Organ and tissue distribution of heavy metals, and their growth-related changes in antarctic fish, pagothenia borchgrevinki. *Agric. Biol. Chem.* **47** (11): 2521–2532. DOI: 10.1080/00021369.1983.10865986.

65. Soudani N, Troudi A, Bouaziz H, Ben Amara I, Boudawara T, Zeghal N (2011) Cardioprotective effects of selenium on chromium (VI)-induced toxicity in female rats. *Ecotoxicol. Environ. Saf.* **74** (3): 513–520. DOI: 10.1016/j.ecoenv.2010.06.009.
66. Kausar H, Singh B, Kaushik RK, Sinha P, Ghai R, Jain S (2017) Protective role of alpha-tocopherol in chromium induced toxicity in albino rat's liver: a histopathological study. *Ann. Int. Med. Dent. Res.* **2** (5): 9–13. DOI: 10.21276/aimdr.2017.3.5.AT2.
67. Kopustinskiene DM, Bernatoniene J (2021) Molecular mechanisms of melatonin-mediated cell protection and signaling in health and disease. *Pharmaceutics* **13** (2): 129. DOI: 10.3390/pharmaceutics13020129.
68. Kocic G, Tomovic K, Kocic H, Sokolovic D, Djordjevic B, Stojanovic S, Arsic I, Smelcerovic A (2017) Antioxidative, membrane protective and antiapoptotic effects of melatonin, in silico study of physico-chemical profile and efficiency of nanoliposome delivery compared to betaine. *RSC Adv.* **7** (3): 1271–1281. DOI: 10.1039/C6RA24741E.
69. Holland SL, Avery S V. (2011) Chromate toxicity and the role of sulfur. *Metallomics* **3** (11): 1119. DOI: 10.1039/c1mt00059d.
70. Patlolla AK, Barnes C, Yedjou C, Velma VR, Tchounwou PB (2009) Oxidative stress, DNA damage, and antioxidant enzyme activity induced by hexavalent chromium in Sprague-Dawley rats. *Environ. Toxicol.* **24** (1): 66–73. DOI: 10.1002/tox.20395.
71. Shrivastava HY, Nair BU (2000) Protein degradation by peroxide catalyzed by chromium (III): role of coordinated ligand. *Biochem. Biophys. Res. Commun.* **270** (3): 749–754. DOI: 10.1006/bbrc.2000.2492.
72. Wang Y, Su H, Gu Y, Song X, Zhao J (2017) Carcinogenicity of chromium and chemoprevention: a brief update. *Onco. Targets. Ther.* **10** : 4065–4079. DOI: 10.2147/OTT.S139262.
73. Jozefczak M, Remans T, Vangronsveld J, Cuypers A (2012) Glutathione is a key player in metal-induced oxidative stress defenses. *Int. J. Mol. Sci.* **13** (3): 3145–3175. DOI: 10.3390/ijms13033145.
74. Soudani N, Ben Amara I, Sefi M, Boudawara T, Zeghal N (2011) Effects of selenium on chromium (VI)-induced hepatotoxicity in adult rats. *Exp. Toxicol. Pathol.* **63** (6): 541–548. DOI: 10.1016/j.etp.2010.04.005.
75. Wiegand HJ, Ottenwälder H, Bolt HM (1984) The reduction of chromium (VI) to chromium (III) by glutathione: An intracellular redox pathway in the metabolism of the carcinogen chromate. *Toxicology* **33** (3–4): 341–348. DOI: 10.1016/0300-483X(84)90050-7.
76. O'Brien T, Xu J, Patierno SR (2001) Effects of glutathione on chromium-induced DNA crosslinking and DNA polymerase arrest. *Mol. Cell. Biochem.* **222** (1–2): 173–182. DOI: 10.1023/A:1017918330073.
77. Menendez-Pelaez A, Reiter RJ (1993) Distribution of melatonin in mammalian tissues: The relative importance of nuclear versus cytosolic localization. *J. Pineal Res.* **15** (2): 59–69. DOI: 10.1111/j.1600-079X.1993.tb00511.x.
78. Ceraulo L, Ferrugia M, Tesoriere L, Segreto S, Livrea MA, Turco Liveri V (1999) Interactions of melatonin with membrane models: Portioning of melatonin in AOT and lecithin reversed micelles. *J. Pineal Res.* **26** (2): 108–112. DOI: 10.1111/j.1600-079X.1999.tb00570.x.
79. Taysi S, Koc M, Büyükokuroğlu ME, Altinkaynak K, Şahin YN (2003) Melatonin reduces lipid peroxidation and nitric oxide during irradiation-induced oxidative injury in the rat liver. *J. Pineal Res.* **34** (3): 173–177. DOI: 10.1034/j.1600-079X.2003.00024.x.
80. Manda K, Ueno M, Anzai K (2007) AFMK, a melatonin metabolite, attenuates X-ray-induced oxidative damage to DNA, proteins and lipids in mice. *J. Pineal Res.* **42** (4): 386–393. DOI: 10.1111/j.1600-079X.2007.00432.x.

81. Gulcin İ, Buyukokuroglu ME, Kufrevioglu OI (2003) Metal chelating and hydrogen peroxide scavenging effects of melatonin. *J. Pineal Res.* **34** (4): 278–281. DOI: 10.1034/j.1600-079X.2003.00042.x.
82. Mitra E, Bhattacharjee B, Pal PK, Ghosh AK, Mishra S, Chattopadhyay A, Bandyopadhyay D (2019) Melatonin protects against cadmium-induced oxidative damage in different tissues of rat: a mechanistic insight. *Melatonin Res.* **2** (2): 1–21. DOI: 10.32794/mr11250018.
83. Sugiyama M (1992) Role of physiological antioxidants in chromium (VI)- induced cellular injury. *Free Radic. Biol. Med.* **12** (5): 397–407. DOI: 10.1016/0891-5849(92)90089-y.
84. Chen L, Zhang J, Zhu Y, Zhang Y (2017) Interaction of chromium(III) or chromium(VI) with catalase and its effect on the structure and function of catalase: An in vitro study. *Food Chem.* **244** : 378–385. DOI: 10.1016/J.FOODCHEM.2017.10.062.
85. Baars AJ, Breimer DD (1980) The glutathione S-transferases. Their role in detoxification and toxification of xenobiotics. *Ann. Biol. Clin. (Paris).* **38** (1): 49–56.
86. Shi X, Dalal NS (1989) Chromium (V) and hydroxyl radical formation during the glutathione reductase-catalyzed reduction of chromium (VI). *Biochem. Biophys. Res. Commun.* **163** (1): 627–634. DOI: 10.1016/0006-291X(89)92183-9.
87. Banerjee S, Joshi N, Mukherjee R, Singh PK, Baxi D, Ramachandran A V. (2017) Melatonin protects against chromium (VI) induced hepatic oxidative stress and toxicity: Duration dependent study with realistic dosage. *Interdiscip. Toxicol.* **10** (1): 20–29. DOI: 10.1515/intox-2017-0003.
88. Cagnoli CM, Atabay C, Kharlamova E, Manev H (1995) Melatonin protects neurons from singlet oxygen-induced apoptosis. *J. Pineal Res.* **18** (4): 222–226. DOI: 10.1111/j.1600-079X.1995.tb00163.x.
89. Mayo JC, Tan DX, Sainz RM, Lopez-Burillo S, Reiter RJ (2003) Oxidative damage to catalase induced by peroxyl radicals: Functional protection by melatonin and other antioxidants. *Free Radic. Res.* **37** (5): 543–553. DOI: 10.1080/1071576031000083206.
90. Marshall KA, Reiter RJ, Poeggeler B, Aruoma OI, Halliwell B (1996) Evaluation of the antioxidant activity of melatonin in vitro. *Free Radic. Biol. Med.* **21** (3): 307–315. DOI: 10.1016/0891-5849(96)00046-9.
91. Matuszak Z, Reszka KJ, Chignell CF (1997) Reaction of melatonin and related indoles with hydroxyl radicals: EPR and spin trapping investigations. *Free Radic. Biol. Med.* **23** (3): 367–372. DOI: 10.1016/S0891-5849(96)00614-4.
92. Zang LY, Cosma G, Gardner H, Vallyathan V (1998) Scavenging of reactive oxygen species by melatonin. *Biochim. Biophys. Acta - Gen. Subj.* **1425** (3): 469–477. DOI: 10.1016/S0304-4165(98)00099-3.
93. Reiter R, Acuna-Castriveijo D, Tan D-X, Burkhardt S (2006) Free radical-mediated molecular damage. *Ann. N. Y. Acad. Sci.* **939** (1): 200–215. DOI: 10.1111/j.1749-6632.2001.tb03627.x.
94. Mayo JC, Sainz RM, Antolín I, Herrera F, Martin V, Rodriguez C (2002) Melatonin regulation of antioxidant enzyme gene expression. *Cell. Mol. Life Sci.* **59** (10): 1706–1713. DOI: 10.1007/PL00012498.
95. Reiter RJ, Tan DX, Carmen O EG (2000) Actions of melatonin in the reduction of oxidative stress. *J. Biomed. Sci.* **7** (6): 444–458. DOI: 10.1007/BF02253360.
96. Chung HY, Baek BS, Song SH, Kim MS, Huh JI, Shim KH, Kim KW, Lee KH (1997) Xanthine dehydrogenase/xanthine oxldase and oxidative stress. *J. Am. Aging Assoc.* **20** (3): 127–140. DOI: 10.1007/s11357-997-0012-2.
97. Kerger BD, Finley BL, Corbett GE, Dodge DG, Paustenbach DJ (1997) Ingestion of chromium(vi) in drinking water by human volunteers: Absorption, distribution, and

excretion of single and repeated doses. *J. Toxicol. Environ. Health*. **50** (1): 67–95. DOI: 10.1080/009841097160618.
98. Wilbur S, Abadin H, Fay M, Yu D, Tencza B, Ingerman L, Klotzbach J, James S (2012)Toxicological Profile for Chromium. Agency for Toxic Substances and Disease Registry (US)(September):1-9.www.atsdr.cdc.gov.
99. Ghosh P, Dey T, Majumder R, Datta M, Chattopadhyay A, Bandyopadhyay D (2023) Insights into the antioxidative mechanisms of melatonin in ameliorating chromium-induced oxidative stress-mediated hepatic and renal tissue injuries in male Wistar rats. *Food Chem. Toxicol.* **173** (113630): 113630. DOI: 10.1016/j.fct.2023.113630.
100. Cabaniss CD. Creatine Kinase. In: Walker HK, Hall WD, Hurst JW, editors. Clinical Methods: The History, Physical, and Laboratory Examinations. 3rd edition. Boston: Butterworths; 1990. Chapter 32. Available from: https://www.ncbi.nlm.nih.gov/books/NBK352/?
101. Selker HP, Zalenski RJ, Antman EM, Aufderheide TP, Bernard SA, Bonow RO, Gibler WB, Hagen MD, Johnson P, Lau J, McNutt RA, Ornato J, Schwartz JS, Scott JD, Tunick PA, Weaver WD (1997) Creatine kinase. *Ann. Emerg. Med.* **29** (1): 59–63. DOI: 10.1016/S0196-0644(97)70308-1.
102. Pritchard J, Ackerman A, Kalyanaraman B (2000) Chromium (VI) increases endothelial cell expression of ICAM-1 and decreases nitric oxide activity. *J. Environ. Pathol. Toxicol. Oncol.* **19** (3): 251–260.
103. Porter R, Jáchymová M, Martásek P, Kalyanaraman B, Vásquez-Vivar J (2005) Reductive activation of Cr(VI) by nitric oxide synthase. *Chem. Res. Toxicol.* **18** (5): 834–843. DOI: 10.1021/tx049778e.
104. Aydogan S, Yerer MB, Goktas A (2006) Melatonin and nitric oxide. *J. Endocrinol. Invest.* **29** (3): 281–287. DOI: 10.1007/BF03345555.
105. Fabrizio RL, Gaia F, Eleonora F, Claudia R, Stefania C, Claudio L, Rita R (2013) Vascular endothelial cells and dysfunctions: role of melatonin. *Front. Biosci. (Elite Ed).* **5** (1): 119–129. DOI: 10.2741/E601.
106. Costa GM, Araujo SL, Xavier Júnior FAF, Morais GB de, Silveira JA de M, Viana D de A, Evangelista JSAM (2019) picrosirius red and masson's trichrome staining techniques as tools for detection of collagen fibers in the skin of dogs with endocrine dermatopathologies. *Ciência Anim. Bras.* **20** (55398): 1–10. DOI: 10.1590/1089-6891v20e-55398.

This work is licensed under a Creative Commons Attribution 4.0 International License

Please cite this paper as:
Ghosh, P., Dey, T., Majumder, R., Datta, M., Chattopadhyay, A. and Bandyopadhyay, D. 2023. Melatonin attenuates chromium-induced oxidative stress-mediated cardiac injury in male Wistar rats: involvement of antioxidative mechanisms. Melatonin Research. 6, 1 (Feb. 2023), 79-101. DOI:https://doi.org/https://doi.org/10.32794/mr112500143.